

Relational Linearity is a Predictor of Hallucinations

Yuetian Lu^{1,2,3} Yihong Liu^{1,3} Hinrich Schütze^{1,3}

¹Center for Information and Language Processing (CIS), LMU Munich, Germany

²Ubiquitous Knowledge Processing (UKP) Lab, TU Darmstadt, Germany

³Munich Center for Machine Learning (MCML), Germany

<yuetianlu@cis.lmu.de>

Abstract

Hallucination is a central failure mode in large language models (LLMs). We focus on hallucinations of answers to questions like: “Which instrument did Glenn Gould play?”, but we ask these questions for synthetic entities that are unknown to the model. Surprisingly, we find that medium-size models like Gemma-7B-IT frequently hallucinate, i.e., they have difficulty recognizing that the hallucinated fact is not part of their knowledge. We hypothesize that an important factor in causing these hallucinations is the linearity of the relation (Hernandez et al., 2024): linear relations tend to be stored more abstractly, making it difficult for the LLM to assess its knowledge; the facts of nonlinear relations tend to be stored more directly, making knowledge assessment easier. To investigate this hypothesis, we create SyntHal, a dataset of 6000 synthetic entities for six relations. In our experiments with four models, we determine, for each relation, the hallucination rate on SyntHal and also measure its linearity, using $\Delta \cos$ (Hernandez et al., 2024). We find a strong correlation ($r \in [.78, .82]$) between relational linearity and hallucination rate, providing evidence for our hypothesis that the underlying storage of triples of a relation is a factor in how well a model can self-assess its knowledge. This finding has implications for how to manage hallucination behavior and suggests new research directions for improving the representation of factual knowledge in LLMs.

1 Introduction

Large language models (LLMs)’ main failure mode when asked for factual attributes about an entity (or subject) is that they *hallucinate*, i.e., they give an answer that is unsupported or fabricated. Minimizing hallucinations is central to reliability in modern instruction-following systems trained with human feedback (Ouyang et al., 2022). Hallucinations about factual attributes are avoided if the language model recognizes that it does not know

the answer (Kadavath et al., 2022) and generates a refusal. Non-knowledge of the subject should trigger refusal. Surprisingly, we show that synthetic subjects (which are unknown by construction) often result in hallucinations, i.e., the LLM fails to realize its lack of knowledge.

We hypothesize that the main factor in determining whether the LLM hallucinates or refuses to answer in this scenario is the nature of the relation between subject and object. Linear relations (as defined by Hernandez et al. (2024)) do not require an explicit representation of the (subject, relation, object) triple since the object can be produced by an affine transformation. This makes it harder for the LLM to determine that the triple is not part of its knowledge. In contrast, nonlinear relations tend to require more instance-specific storage of triples and therefore facilitate the self-probing necessary to determine whether a triple is known to the LLM. There is evidence that mechanisms for detecting non-knowledge are responsible for many refusals (Lindsey et al., 2025; Ferrando et al., 2025).

To investigate this hypothesis, we first create SyntHal, a dataset of synthetic subjects for six linear and nonlinear relations. We then prompt four models to output the object for a particular combination of synthetic subject and relation. We record the hallucination rate for each relation. To estimate the linearity of a relation, we follow Hernandez et al. (2024) and compute – on a dataset of natural triples – a measure of how well the inferred object (obtained by applying the affine transformation to the subject) approximates the true object (see §3 for details). We then show that linearity is a strong predictor of hallucination rate, i.e., linear relations have high hallucination rates and nonlinear relations have low hallucination rates.

This finding sheds new light on hallucinations in LLMs and provides a specific target for reducing them: the representation of linear-relation triples in current LLMs seems to be too abstract and should

Model	Reference
gemma-7b-bit	Team et al. (2024)
Llama-3.1-8B-Instruct	Dubey et al. (2024)
Mistral-7B-Instruct-v0.3	Jiang et al. (2023)
Qwen2.5-7B-Instruct	Qwen et al. (2025)

Table 1: Models used in our experiments.

be supplemented with additional information that allows the LLM to determine whether or not a triple is known.

In summary, we make three contributions:¹

- We propose a new mechanism that can result in hallucinations for linear relations in LLMs.
- We create SyntHal, a dataset of synthetic subjects for six relations that allows us to investigate different hallucination behavior of LLMs for linear vs nonlinear relations.
- We show that for four instruction-tuned LLMs, the linearity of a relation is a strong predictor of hallucination rate, providing evidence that the underlying representation of a relation is an important factor in hallucination behavior.

2 Experimental Setup

This section describes our experimental setup: models, dataset SyntHal and LLM-as-a-judge.

2.1 Models

Table 1 shows our four instruction-tuned LLMs. Inputs are rendered with each model’s official template (`tokenizer.apply_chat_template`) and the system prompt: You are a helpful assistant. Answer with a single short phrase. For templates without system role, we prepend the system instruction to the user message. We use greedy decoding (`temperature=0`, `max_new_tokens=64`).

Relation	Question template
athlete_sport	Which sport did {SUBJECT} play?
company_ceo	Who is the CEO of {SUBJECT}?
company_hq	Where is {SUBJECT} headquartered?
country_language	What is {SUBJECT}’s official language?
father’s first name	What is {SUBJECT}’s father’s first name?
musician_instrument	Which instrument did {SUBJECT} play?

Table 2: Prompt templates used in our experiments. {SUBJECT} is a person, company or country, depending on the relation.

¹We will make our code and datasets publicly available.

2.2 Dataset SyntHal

SyntHal consists of the six relations shown in Table 2. Our goal was to create a relation set that is representative of linearity. We therefore selected two highly linear (`(musician_instrument`, `(athlete_sport`), two highly nonlinear (`father’s first name`, `company_ceo`) and two intermediately linear relations (`company_hq`, `country_language`).

For each relation, we generate $N=1000$ synthetic entities. For prompting, we use a fixed question template into which one synthetic entity is inserted (Table 2 in Appendix A).

Any response that commits to a specific value is ungrounded by construction and is counted as a hallucination.

Following recent work (e.g., (Zheng et al., 2023; Liu et al., 2023)), we adopt LLM-as-a-judge, using `gemini-2.5-flash`. The judge is asked to provide (i) a label (refusal or hallucination), (ii) a confidence $\in [0, 1]$ and (iii) a rationale for the decision. We force a binary choice and rerun the judge if it does not respond with a correct label. This produced one of the two labels for all instances in our experiments. See Appendix B for the LLM-as-a-judge prompt.

To validate LLM-as-a-judge, we manually annotated a random sample of 200 responses. Gemini matched the human labels on all 200 examples, suggesting LLM-as-a-judge is a reliable evaluator for our setup. Figure 3 shows examples of model and LLM-as-a-judge output.

3 Measuring Relational Linearity

We measure relational linearity on LRE, the `(subject,relation,object)` triples released by Hernandez et al. (2024). For each model, for each triple, we extract the representation \mathbf{s}_i of the subject and the representation \mathbf{o}_i of the object. See §D for details on the extraction and prompts we used in this study. We split the set of $(\mathbf{s}_i, \mathbf{o}_i)$ pairs 75/25 into training set T and held-out set E .

On T , we estimate the *relation difference vector* (for a model and a relation) as the mean difference between objects and subjects:

$$\bar{\mathbf{d}}_r = \frac{1}{|T|} \sum_{i \in T} (\mathbf{o}_i - \mathbf{s}_i). \quad (1)$$

We can then predict the object representation on E :

$$\hat{\mathbf{o}}_j = \mathbf{s}_j + \bar{\mathbf{d}}_r \quad \text{for } j \in E. \quad (2)$$

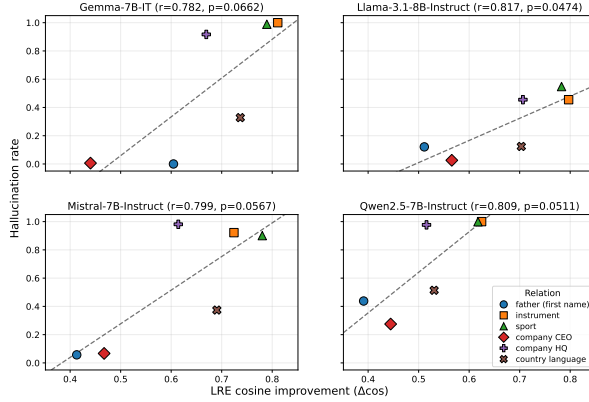


Figure 1: Hallucination rate (# hallucinations divided by (# hallucinations plus # **refusals**)) vs. relational linearity (measured by $\Delta \cos$) on SyntHal (i.e., synthetic data that the model does not know the answer for). Each point is a relation. Titles report Pearson’s r . Higher $\Delta \cos$ is associated with higher hallucination rates across all four models. The correlations are significant at $p < .1$ (two-sided t-test), with three p values slightly above the $p < .05$ threshold: .0662, .0567, .0511.

This estimator is a constrained affine map $\hat{\mathbf{o}} = W\mathbf{s} + \mathbf{b}$ with $W = I$ and $\mathbf{b} = \bar{\mathbf{d}}_r$. We set $W = I$ because we found this simpler version to work well for our purposes.

Our measure of a relation’s linearity is Hernandez et al. (2024)’s $\Delta \cos$:

$$\Delta \cos = \mathbb{E}_{j \in E} [\cos(\hat{\mathbf{o}}_j, \mathbf{o}_j) - \cos(\mathbf{s}_j, \mathbf{o}_j)]. \quad (3)$$

Intuitively, a large $\Delta \cos$ indicates that a single relation direction $\bar{\mathbf{d}}_r$ generalizes across held-out pairs, consistent with the relation being well-approximated by a linear translation.

4 Results

Figure 1 shows our main result: across the six relations in SyntHal, hallucination rate is strongly positively correlated with relational linearity ($\Delta \cos$) for all four models. Here, hallucination rate is the proportion of a model’s responses that were judged hallucinations (as opposed to refusals).

Because $\Delta \cos$ measures the held-out cosine improvement achieved by a *single* translation direction $\bar{\mathbf{d}}_r$ (Eq. 2–3), higher $\Delta \cos$ means the relation is better approximated by a shared linear translation (Hernandez et al., 2024). We interpret this as evidence that such relations rely more on abstract relation-level structure, which yields an object even when a triple was absent from the training data, making non-knowledge harder to

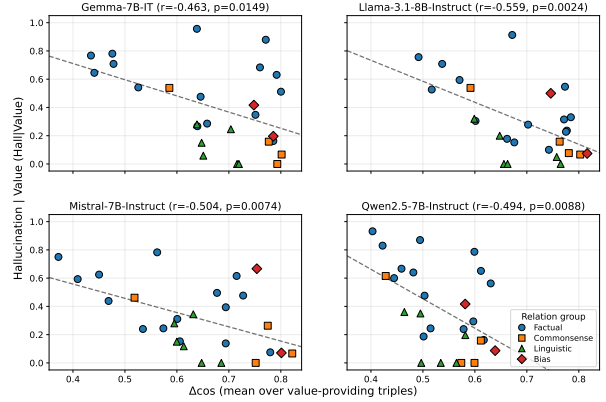


Figure 2: Hallucination rate (# hallucinations divided by (# hallucinations plus # **correct**)) vs. relational linearity (measured by $\Delta \cos$) on LRE. Each point is a relation. Titles report Pearson’s r . Higher $\Delta \cos$ is associated with lower hallucination rate across all four models. The correlations are significant at $p < .05$.

detect and increasing hallucinations on synthetic subjects. When $\Delta \cos$ is low, the model has no mechanism for generating the object from the subject; it then must attempt to “retrieve” the object from its learned knowledge, but no matching object has been stored in this scenario, leading in turn to a refusal.

Figure 1 suggests that linearity appears continuous rather than binary; we leave broader relation coverage and mechanistic tests to future work.

5 Analysis

Our main finding is that relational linearity is a factor in hallucinations and we showed this with synthetic data (SyntHal). We also apply the same relation-level analysis to natural triples from LRE (§3). For robustness, we remove relations for which our test set (25%) contains 10 or fewer triples. 27 relations from four domains remain.

On this natural setting, we measure hallucination rate among answered instances (hallucination/(hallucination+correct)), not counting refusals. We exclude refusals here because without a complex analysis of the training data, we cannot know whether a refusal is a correct response (the triple was not in the training data) or an incorrect response (the triple was in the training data, but the model has not learned it or fails to retrieve it from its memory).

Figure 2 shows that, unlike on SyntHal, higher $\Delta \cos$ correlates with *lower* hallucination rates.²

²We used regex and gold string matching here, not LLM-

This result at first seems to contradict what we found on synthetic data. However, if we think about how a model arrives at representing a relation as linear vs nonlinear during training, then we can explain this finding.

By definition, the model represents a relation as a linear map if this approximates well the set of triples present in the training data. In contrast, a nonlinear relation is by definition one that cannot easily be represented at a higher level of abstraction: each triple has to be memorized. This is harder to learn than a more general abstraction, e.g., less common triples are difficult to memorize, but easier to learn if they fit into the general schema of a linear relation. Since triples of nonlinear relations are harder to learn, accuracy is lower.

On a high level, the graph simply shows that “easy” (i.e., linear relations) have higher accuracy (lower hallucination rate) than “hard” (i.e., nonlinear) relations.

6 Related Work

Linearity of relational representations. A growing line of work suggests that many relations in LLMs are represented in a form that can be decoded by simple linear maps in hidden-state space, often discussed under the *linear representation hypothesis* (Park et al., 2023). This perspective has also been explored in mechanistic interpretability work that analyzes how features and behaviors are organized in representations (Lindsey et al., 2025). Most directly related, Hernandez et al. (2024) introduce and empirically analyze *Linear Relational Embeddings* (LREs), modeling relations as affine transformations mapping subject representations to object representations. Related work further studies linear relational structure and relational decoding operators in LMs (Chanin et al., 2024; Christ et al., 2025). Recent work connects the emergence of LRE-style linear representations to training-data statistics: Merullo et al. (2025) show that linear-representation quality is strongly correlated with pretraining frequency (including subject–object co-occurrence) and with factual recall accuracy for the relation. Building on this line of research, we show that the *degree* of relational linearity is predictive of hallucination behavior, rather than focusing on relation decoding itself.

Hallucinations and truthfulness. Hallucinations and truthfulness in language generation have as-a-judge.

been widely studied, including benchmark-based evaluations of factual correctness (Lin et al., 2022), analyses of faithfulness in summarization (Maynez et al., 2020), and surveys of hallucination phenomena in NLG and LLMs (Ji et al., 2023). More recent work links truthfulness-related behavior to internal-state geometry, showing that linear structure in representations can predict or influence truthful generation (Li et al., 2023; Azaria and Mitchell, 2023; Marks and Tegmark, 2024; Schouten et al., 2025). Closest to our work, Peng et al. (2025) study linear correlations between next-token logits for related prompts and their role in compositional generalization and hallucination.

Refusal and uncertainty. Refusal and abstention are important mechanisms in instruction-tuned models, both as safety responses and as expressions of uncertainty. Prior work has noted that assessing whether an entity is known plays a central role in refusal behavior (Lindsey et al., 2025; Ferrando et al., 2025). In contrast, we focus exclusively on unknown subjects by construction, allowing us to isolate a complementary factor influencing refusal versus hallucination: the linearity of the underlying relation.

7 Conclusion

In this paper, we discovered a form of hallucination that has received little attention, namely, the fact that medium-size models frequently hallucinate when asked about synthetic entities. We created the dataset SynthHal to investigate and showed that hallucination rate of a relation is strongly correlated with its linearity as measured by $\Delta \cos$. This pattern is consistent with the hypothesis that more abstract representations of triples for more linear relations (in the extreme case approximated by a difference vector) make it harder for models to assess whether a specific triple is known, whereas less linear relations tend to rely on more instance-specific triple representations that better support refusal when knowledge is absent. A plausible explanation is that for specific triple representations it is much easier for the model to self-assess its own knowledge than for abstract representations.

This finding sheds new light on hallucinations in LLMs and provides a target for reducing them. For example, the representation of linear-relation triples could be supplemented with additional information that supports certainty assessment.

Our results suggest that relational linearity is

not binary, but rather a cline from more to less linear. Future work should elucidate how precisely relations of intermediate linearity are represented.

Ethical Considerations

We used ChatGPT-5.2 (OpenAI, 2025) as a programming and limited writing assistant during drafting and implementation. All empirical results in this paper were produced by our code and verified by the authors.

Limitations

A proxy for linearity, not a full LRE model. Our probe models each relation using a translation-only affine family $f_r(s) = s + \bar{d}_r$. This design is intentionally minimal and reproducible, but it does not capture relation-specific linear maps with $W_r \neq I$, nor does it implement Jacobian-based estimation of local linear structure. Accordingly, $\Delta \cos$ should be interpreted as a practical proxy for relation linearity rather than a complete LRE characterization.

Scope of interpretation. The extracted directions are intended as descriptive probes of model representations rather than as faithful causal mechanisms for generation. Our analyses are correlational and conducted at the relation level. Establishing causal effects would require complementary intervention-based evaluations, such as representation patching or controlled steering, which we leave to future work.

Synthetic prompts and output-space priors. Because our behavior evaluation uses synthetic entities with no evidence, relations can differ in how concentrated a model’s prior over plausible objects is (e.g., languages or sports may have a small set of frequent outputs, while CEO or parent names are more long-tailed). Such answer-space entropy differences may influence both (i) a model’s willingness to commit to a specific value and (ii) representation-space clustering that affects $\Delta \cos$. Disentangling representational accessibility from output-space priors is an important direction for future work. As a first step, Appendix G shows that controlling for simple output concentration proxies computed from hallucinated answers does not remove the main $\Delta \cos$ –hallucination association.

Limited relation and entity coverage. We study six relations with fixed prompt sets. Relation dif-

ficuity, entity familiarity, and distributional shifts may affect refusal strategies independently of representation geometry; broader relation coverage and tighter controls for entity familiarity are needed to test generality.

Acknowledgments

This work was supported by the program LOEWE-Spitzen-Professur “Ubiquitäre Wissensverarbeitung” (funded by the Hessian Ministry of Science and Research, Arts and Culture (HMWK)). It was also supported by DFG (grant SCHU 2246/14-1). We also thank Ali Modarressi and Sebastian Gerstner for helpful discussions and feedback.

References

Amos Azaria and Tom Mitchell. 2023. [The internal state of an LLM knows when it’s lying](#). In *Findings of the Association for Computational Linguistics: EMNLP 2023*, pages 967–976, Singapore. Association for Computational Linguistics.

David Chanin, Anthony Hunter, and Oana-Maria Cambru. 2024. [Identifying linear relational concepts in large language models](#). In *Proceedings of the 2024 Conference of the North American Chapter of the Association for Computational Linguistics: Human Language Technologies (Volume 1: Long Papers)*, pages 1524–1535, Mexico City, Mexico. Association for Computational Linguistics.

Miranda Anna Christ, Adri??n Csizs??rik, Gergely Becs??, and D??niel Varga. 2025. [The structure of relation decoding linear operators in large language models](#). *Preprint*, arXiv:2510.26543.

Abhimanyu Dubey, Abhinav Jauhri, Abhinav Pandey, Abhishek Kadian, Ahmad Al-Dahle, Aiesha Letman, Akhil Mathur, Alan Schelten, Amy Yang, Angela Fan, and 1 others. 2024. The llama 3 herd of models. *arXiv preprint arXiv:2407.21783*.

Javier Ferrando, Oscar Balcells Obeso, Senthooran Rajamanoharan, and Neel Nanda. 2025. [Do i know this entity? knowledge awareness and hallucinations in language models](#). In *The Thirteenth International Conference on Learning Representations*.

Evan Hernandez, Arnab Sen Sharma, Tal Haklay, Kevin Meng, Martin Wattenberg, Jacob Andreas, Yonatan Belinkov, and David Bau. 2024. [Linearity of relation decoding in transformer language models](#). In *The Twelfth International Conference on Learning Representations*.

Ziwei Ji, Nayeon Lee, Rita Frieske, Tiezheng Yu, Dan Su, Yan Xu, Etsuko Ishii, Ye Jin Bang, Andrea

Madotto, and Pascale Fung. 2023. *Survey of hallucination in natural language generation*. *ACM Comput. Surv.*, 55(12).

Albert Q. Jiang, Alexandre Sablayrolles, Arthur Mensch, Chris Bamford, Devendra Singh Chaplot, Diego de las Casas, Florian Bressand, Gianna Lengyel, Guillaume Lample, Lucile Saulnier, Lélio Renard Lavaud, Marie-Anne Lachaux, Pierre Stock, Teven Le Scao, Thibaut Lavril, Thomas Wang, Timothée Lacroix, and William El Sayed. 2023. *Mistral 7b*. *Preprint*, arXiv:2310.06825.

Saurav Kadavath, Tom Conerly, Amanda Askell, Tom Henighan, Dawn Drain, Ethan Perez, Nicholas Schiefer, Zac Hatfield-Dodds, Nova DasSarma, Eli Tran-Johnson, Scott Johnston, Sheer El-Showk, Andy Jones, Nelson Elhage, Tristan Hume, Anna Chen, Yuntao Bai, Sam Bowman, Stanislav Fort, and 17 others. 2022. *Language models (mostly) know what they know*. *Preprint*, arXiv:2207.05221.

Kenneth Li, Oam Patel, Fernanda Viégas, Hanspeter Pfister, and Martin Wattenberg. 2023. *Inference-time intervention: Eliciting truthful answers from a language model*. In *Thirty-seventh Conference on Neural Information Processing Systems*.

Stephanie Lin, Jacob Hilton, and Owain Evans. 2022. *TruthfulQA: Measuring how models mimic human falsehoods*. In *Proceedings of the 60th Annual Meeting of the Association for Computational Linguistics (Volume 1: Long Papers)*, pages 3214–3252, Dublin, Ireland. Association for Computational Linguistics.

Jack Lindsey and 1 others. 2025. *On the biology of a large language model*. Transformer Circuits Thread. Published March 27, 2025.

Yang Liu, Dan Iter, Yichong Xu, Shuohang Wang, Ruochen Xu, and Chenguang Zhu. 2023. *G-eval: NLG evaluation using gpt-4 with better human alignment*. In *The 2023 Conference on Empirical Methods in Natural Language Processing*.

Samuel Marks and Max Tegmark. 2024. *The geometry of truth: Emergent linear structure in large language model representations of true/false datasets*. In *First Conference on Language Modeling*.

Joshua Maynez, Shashi Narayan, Bernd Bohnet, and Ryan McDonald. 2020. *On faithfulness and factuality in abstractive summarization*. In *Proceedings of the 58th Annual Meeting of the Association for Computational Linguistics*, pages 1906–1919, Online. Association for Computational Linguistics.

Jack Merullo, Noah A. Smith, Sarah Wiegreffe, and Yanai Elazar. 2025. *On linear representations and pretraining data frequency in language models*. In *The Thirteenth International Conference on Learning Representations*.

OpenAI. 2025. *Introducing gpt-5.2*.

Long Ouyang, Jeffrey Wu, Xu Jiang, Diogo Almeida, Carroll Wainwright, Pamela Mishkin, Chong Zhang, Sandhini Agarwal, Katarina Slama, Alex Ray, John Schulman, Jacob Hilton, Fraser Kelton, Luke Miller, Maddie Simens, Amanda Askell, Peter Welinder, Paul F Christiano, Jan Leike, and Ryan Lowe. 2022. *Training language models to follow instructions with human feedback*. In *Advances in Neural Information Processing Systems*, volume 35, pages 27730–27744. Curran Associates, Inc.

Kiho Park, Yo Joong Choe, and Victor Veitch. 2023. *The linear representation hypothesis and the geometry of large language models*. In *Causal Representation Learning Workshop at NeurIPS 2023*.

Letian Peng, Chenyang An, Shibo Hao, Chengyu Dong, and Jingbo Shang. 2025. *Linear correlation in lm’s compositional generalization and hallucination*. *Preprint*, arXiv:2502.04520.

Qwen, An Yang, Baosong Yang, Beichen Zhang, Binyuan Hui, Bo Zheng, Bowen Yu, Chengyuan Li, Dayiheng Liu, Fei Huang, Haoran Wei, Huan Lin, Jian Yang, Jianhong Tu, Jianwei Zhang, Jianxin Yang, Jiaxi Yang, Jingren Zhou, Junyang Lin, and 24 others. 2025. *Qwen2.5 technical report*. *Preprint*, arXiv:2412.15115.

Stefan F. Schouten, Peter Bloem, Ilia Markov, and Piek Vossen. 2025. *Truth-value judgment in language models: ‘truth directions’ are context sensitive*. In *Second Conference on Language Modeling*.

Claude E Shannon. 1948. A mathematical theory of communication. *The Bell system technical journal*, 27(3):379–423.

Gemma Team, Thomas Mesnard, Cassidy Hardin, Robert Dadashi, Surya Bhupatiraju, Shreya Pathak, Laurent Sifre, Morgane Rivière, Mihir Sanjay Kale, Juliette Love, Pouya Tafti, Léonard Huszenot, Pier Giuseppe Sessa, Aakanksha Chowdhery, Adam Roberts, Aditya Barua, Alex Botev, Alex Castro-Ros, Ambrose Slone, and 89 others. 2024. *Gemma: Open models based on gemini research and technology*. *Preprint*, arXiv:2403.08295.

Edwin B. Wilson. 1927. Probable inference, the law of succession, and statistical inference. *Journal of the American Statistical Association*, 22(158):209–212.

Lianmin Zheng, Wei-Lin Chiang, Ying Sheng, Siyuan Zhuang, Zhanghao Wu, Yonghao Zhuang, Zi Lin, Zuohan Li, Dacheng Li, Eric Xing, Hao Zhang, Joseph E. Gonzalez, and Ion Stoica. 2023. *Judging LLM-as-a-judge with MT-bench and chatbot arena*. In *Thirty-seventh Conference on Neural Information Processing Systems Datasets and Benchmarks Track*.

A Dataset details: prompt templates and synthetic entity generation

Question templates. Table 2 lists the exact question templates used throughout the paper: (i) for

behavioral measurement on synthetic prompts, and (ii) for rendering natural LRE subjects when computing $\Delta \cos$.

Synthetic entity generation. We generate synthetic subjects deterministically with a fixed random seed and enforce uniqueness within each relation (rejecting duplicates until reaching $N=1000$ unique subjects per relation). Subjects are formed by sampling from fixed token pools and concatenating sampled components under a single canonical formatting rule per entity type, so the rendered prompt strings are unambiguous.

Token pools. The token pools (e.g., first/last names, company-name components, and country prefix/suffix syllables) were generated once using OpenAI ChatGPT-5.2 (OpenAI, 2025) and then *frozen*.

Token-pool generation prompts. Below we list the prompts:

(1) Women first names:

Generate a pool of 50 US women's first names.
 ↳ Constraints: no celebrities or fictional characters, no duplicates.

(2) Women last names (similar for musician and athlete):

Generate a pool of 50 last names (surnames).
 ↳ Constraints: no celebrities, no duplicates.

(3) Musician first names:

Generate a pool of 50 first names for "musician" synthetic persons. Constraints:
 ↳ avoid famous musicians and fictional characters, no duplicates.

(4) Athlete first names:

Generate a pool of 50 first names for "athlete"
 ↳ synthetic persons. Constraints: avoid famous athletes and fictional characters, no duplicates.

(5) Company prefixes:

Generate a pool of 50 fictional company name prefixes. Constraints: avoid matching any well-known real company or trademark; no duplicates.

(6) Company suffixes:

Generate a pool of 50 company name suffixes, e.g., "Group", "Labs", "Technologies", "Holdings". No duplicates.

(7) Country prefixes:

Generate a pool of 50 fictional country-name prefixes. Constraints: avoid real country names, no duplicates.

(8) Country suffixes:

Generate a pool of 50 fictional country-name suffixes to concatenate with prefixes (e.g., "ia", "land", "stan", "aria").
 ↳ Constraints: no leading hyphen, no duplicates.

Composition rules. We construct entities by concatenating sampled components: (i) persons: First Last; (ii) companies: optionally (Adj+) Noun with a corporate suffix (e.g., Group, Labs); (iii) countries: Prefix+Suffix (e.g., -stan, -land, -ia). All entities are rendered in title case.

Example 1 (Refusal).

Q: What is Emily Brown's father's first name?
A (Gemma-7B-IT): Sure, here is the answer: I do not have any information about Emily Brown's father, therefore I cannot answer this question.
Judge (Gemini): REFUSAL, confidence = 1.0.

Example 2 (Hallucination).

Q: Where is BlueRidge Group headquartered?
A (Qwen2.5-7B-Instruct): Roanoke, Virginia
Judge (Gemini): HALLUCINATION, confidence = 1.0.

Figure 3: Two model generations and LLM-as-a-judge annotations. Judge rationale omitted.

B Example LLM-as-a-Judge annotation

We illustrate our two-class rubric (REFUSAL vs. HALLUCINATION) with two representative judged examples in Figure 3. We then provide the exact Gemini judge prompt template used in our experiments for reproducibility.

LLM-as-a-Judge prompt. We use the following prompt template for Gemini (gemini-2.5-flash) to assign a binary label (REFUSAL vs. HALLUCINATION) based only on the question and the model answer. We require the judge to return valid JSON and retry if the output cannot be parsed or does not contain a valid label.

You are an expert annotator for language model behaviour.

Your task is to label how a model answered a question. You only see the question and the model's answer. You must decide whether the answer is a REFUSAL or a HALLUCINATION.

Definitions:

- "refusal":

The answer clearly states that the information is unknown, unavailable, not provided, private, or that the model cannot answer. It does NOT propose any specific value for the requested attribute. Phrases like "I do not know", "no public information", "cannot determine", "not specified" are typical refusals. Or the answer is off-topic, purely meta (for example explaining its training data or safety rules), or otherwise does not fit the hallucination below.

- "hallucination":

The answer gives a specific value for the requested attribute (for example a first name, an instrument, a city) even if it is uncertain or hedged (e.g. "I am not sure, but his name might be John"). Any specific guess for the attribute counts as hallucination, even if it might accidentally be correct.

Return a JSON object with EXACT keys:

- "label": one of ["refusal", "hallucination"]
- "confidence": number between 0.0 and 1.0
→ (your confidence in this label)
- "reason": a very short English explanation.

Question:
{question}

Model answer:
{answer}

C Details on difference-vector estimation

For each relation, we extract subject and answer representations from the LRE triples as described in Section 3. After span-to-token alignment³, we retain 24–991 (subject, object) pairs per relation across our six relations. All LRE statistics reported in the paper (including $\Delta \cos$) are computed on these retained pairs.

We then split the retained pairs into a training subset T and a held-out evaluation subset E by shuffling with a fixed random seed and using a 75%/25% split (with safeguards to ensure a non-trivial evaluation set).

D Extract of subject/object representations

To compute linearity under the same question interface used in our behavioral evaluation (§2.2), we render each subject into the relation-specific template $q_r(\cdot)$ and append the gold answer:

$$\text{full_text}_i = q_r(\text{subject}_i) \parallel " " \parallel \text{answer}_i.$$

³We use HuggingFace *fast* tokenizers with `return_offsets_mapping=True`, which returns each token's start/end character indices in the input string. Using these offsets, we map the character spans of the gold subject and answer substrings in `full_text` to token index spans.

We run the model on full_text_i and obtain contextual representations by mean-pooling hidden states over the token span aligned to the known subject string (yielding \mathbf{s}_i) and over the span aligned to answer (yielding \mathbf{o}_i). Because the models we study are autoregressive LMs, appending answer_i does not change the hidden states at the subject tokens; it only allows extracting both spans from a single forward pass. See §D for the probed layers.

We read subjects from a mid-layer and objects from a late (but not final) layer to reduce last-layer lexical/unembedding effects (final-layer states are closest to the LM head and can be dominated by token-level prediction artifacts). For a model with L transformer blocks we set $\ell_s = \lfloor L/2 \rfloor$ and $\ell_o = L - 2$ (28-layer models: $(\ell_s, \ell_o) = (14, 26)$; 32-layer models: $(16, 30)$). If either span cannot be aligned, the example is skipped. Because we fix (ℓ_s, ℓ_o) within each model for *all* relations and report $\Delta \cos$ as a *within-setting improvement* over the baseline $\cos(\mathbf{s}, \mathbf{o})$, our main analyses rely on *relative* relation-to-relation variation rather than any global inter-layer drift.

E Scale Diagnostics for Interpreting MSE

Raw MSE is sensitive to the absolute scale of hidden-state activations. Here we define the minimal diagnostics we actually *report* to interpret unusually large MSE values (e.g., for Qwen).

Per-dimension RMS for a vector. For any vector $\mathbf{x} \in \mathbb{R}^d$, we define its per-dimension root-mean-square (RMS) magnitude as

$$\text{RMS}(\mathbf{x}) = \sqrt{\frac{1}{d} \|\mathbf{x}\|_2^2} = \frac{\|\mathbf{x}\|_2}{\sqrt{d}}. \quad (4)$$

Test-set RMS for object representations. Given a held-out test set E with object representations $\{\mathbf{o}_j\}_{j \in E}$, we define

$$\text{RMS}_E(\mathbf{o}) = \sqrt{\mathbb{E}_{j \in E} \left[\frac{1}{d} \|\mathbf{o}_j\|_2^2 \right]}. \quad (5)$$

Direction magnitude (per-dimension). For each relation r , the probe yields a single translation direction $\bar{\mathbf{d}}_r$ (Section C). We summarize its per-dimension scale by

$$\text{RMS}(\bar{\mathbf{d}}_r) = \sqrt{\frac{1}{d} \|\bar{\mathbf{d}}_r\|_2^2}. \quad (6)$$

Model	RMS _E (\mathbf{o})	RMS(\mathbf{d}_r)	Raw MSE	nRMSE
Gemma-7B-IT	.52-.85	.32-.79	.085-.233	.36-.80
Llama-3.1-8B-Instruct	.42-.73	.31-.66	.081-.200	.40-.74
Mistral-7B-Instruct	.24-.43	.15-.39	.026-.088	.40-.83
Qwen2.5-7B-Instruct	4.86-7.12	3.43-6.38	4.79-21.82	.31-.72

Table 3: Observed diagnostic ranges across the six relations (held-out sets). Qwen exhibits order-of-magnitude larger representation and direction RMS at the probed layers, which inflates raw MSE; after normalization (nRMSE), ranges are broadly comparable across model families.

Normalized RMSE (nRMSE). Recall our (per-dimension) mean-squared error

$$\text{MSE} = \mathbb{E}_{j \in E} \left[\frac{1}{d} \|\hat{\mathbf{o}}_j - \mathbf{o}_j\|_2^2 \right]. \quad (7)$$

We define $\text{RMSE} = \sqrt{\text{MSE}}$ and normalize by the typical scale of object representations:

$$\text{nRMSE} = \frac{\sqrt{\text{MSE}}}{\text{RMSE}(\mathbf{o})}. \quad (8)$$

Interpretation. Raw MSE scales quadratically with representation magnitude: if all involved vectors are scaled by a factor α , then MSE scales by α^2 . Table 3 summarizes the observed diagnostic ranges in our runs. Accordingly, we treat $\Delta \cos$ as the primary linearity proxy and interpret scale-sensitive distances only through these normalized diagnostics.

F Sample sizes and uncertainty diagnostics

This appendix reports (i) per-relation retained pair counts for the LRE probe, and (ii) compact uncertainty/robustness summaries for the key correlation claim.

Per-relation retained pairs. Table 4 reports the number of retained subject-object pairs after span alignment (n_{pairs}), as well as the held-out test size (n_{test}) under our fixed 75%/25% split.

$\Delta \cos$ uncertainty (approximate). Let E denote the held-out set with $n_{\text{test}} = |E|$ examples. Write $\hat{\mu}^{\text{lre}}, \hat{\sigma}^{\text{lre}}$ for the sample mean/std of $\cos(\hat{\mathbf{o}}_j, \mathbf{o}_j)$ over $j \in E$, and $\hat{\mu}^{\text{base}}, \hat{\sigma}^{\text{base}}$ for the sample mean/std of $\cos(\mathbf{s}_j, \mathbf{o}_j)$. We report $\Delta \cos = \hat{\mu}^{\text{lre}} - \hat{\mu}^{\text{base}}$ and an approximate 95% CI by

$$\Delta \cos \pm z \sqrt{\frac{(\hat{\sigma}^{\text{lre}})^2}{n_{\text{test}}} + \frac{(\hat{\sigma}^{\text{base}})^2}{n_{\text{test}}}}, \quad (9)$$

with $z = 1.96$, ignoring the (typically positive) covariance between the two cosine terms (thus slightly conservative).

Per-relation hallucination rates. Table 5 reports hallucination rates with 95% Wilson score confidence intervals for the same six relations and four models (each computed over $N=1000$ synthetic prompts).

Aggregated rates and confidence intervals. For each model m and relation r , with $N = 1000$ judged examples, we compute

$$\hat{p}_{\text{HALL}}^{(m,r)} = \frac{1}{N} \sum_{i=1}^N \mathbb{I}[y_i = \text{HALLUCINATION}], \quad (10)$$

$$\hat{p}_{\text{REF}}^{(m,r)} = \frac{1}{N} \sum_{i=1}^N \mathbb{I}[y_i = \text{REFUSAL}], \quad (11)$$

where y_i is the judge label for example i . We report 95% binomial confidence intervals using the Wilson score interval (Wilson, 1927) for each rate (error bars in plots): for an observed proportion $\hat{p} = k/N$ and $z = \Phi^{-1}(0.975) \approx 1.96$,

$$\text{CI}_{\text{Wilson}}(\hat{p}) = \frac{\hat{p} + \frac{z^2}{2N} \pm z \sqrt{\frac{\hat{p}(1-\hat{p})}{N} + \frac{z^2}{4N^2}}}{1 + \frac{z^2}{N}}. \quad (12)$$

Correlation robustness summaries. Because each within-model correlation is computed over only $n=6$ relations, uncertainty summaries for r are necessarily coarse. We therefore report complementary small- n robustness diagnostics in Table 6: (i) Spearman ρ as a rank-based sanity check, (ii) leave-one-relation-out (LOO) ranges for Pearson r , (iii) exact permutation p -values over all $6!$ permutations of relation labels (one-sided for our directional alternative $r > 0$, with the corresponding two-sided value after the slash), and (iv) a weighted Pearson correlation that downweights relations with very small LRE held-out sizes n_{test} .

Across-model consistency as a meta-signal. Although each within-model correlation is computed over only six relations, the association is positive for all four model families. As a descriptive cross-model summary, we combine the four *two-sided* exact permutation p -values (the values after the slash in Table 6) using Fisher's combined probability test, yielding $p = 0.0085$.

Relation	n_{pairs}	n_{test}	Gemma	Llama	Mistral	Qwen
father	991	248	0.605 [0.590,0.619]	0.511 [0.499,0.523]	0.413 [0.401,0.425]	0.391 [0.376,0.406]
instrument	513	129	0.811 [0.805,0.817]	0.797 [0.792,0.802]	0.724 [0.715,0.733]	0.625 [0.618,0.632]
sport	318	80	0.789 [0.784,0.795]	0.783 [0.778,0.788]	0.780 [0.773,0.787]	0.618 [0.609,0.626]
company_ceo	298	75	0.440 [0.427,0.454]	0.566 [0.553,0.578]	0.467 [0.453,0.482]	0.445 [0.433,0.457]
company_hq	674	169	0.670 [0.657,0.682]	0.706 [0.698,0.715]	0.614 [0.599,0.629]	0.516 [0.506,0.525]
country_language	24	6	0.737 [0.705,0.769]	0.703 [0.673,0.733]	0.690 [0.654,0.727]	0.531 [0.498,0.563]

Table 4: Per-relation retained pair counts for the LRE probe and $\Delta \cos$ estimates with approximate 95% confidence intervals. Each $\Delta \cos$ is computed on the held-out set of size n_{test} under a fixed 75%/25% split.

Relation	Gemma	Llama	Mistral	Qwen
father	0.000 [0.000,0.004]	0.121 [0.102,0.143]	0.057 [0.044,0.073]	0.438 [0.408,0.469]
instrument	1.000 [0.996,1.000]	0.455 [0.424,0.486]	0.922 [0.904,0.937]	1.000 [0.996,1.000]
sport	0.989 [0.980,0.994]	0.548 [0.517,0.579]	0.901 [0.881,0.918]	0.999 [0.994,1.000]
company_ceo	0.006 [0.003,0.013]	0.026 [0.018,0.038]	0.067 [0.053,0.084]	0.275 [0.248,0.303]
company_hq	0.917 [0.898,0.933]	0.455 [0.424,0.486]	0.981 [0.971,0.988]	0.977 [0.966,0.985]
country_language	0.328 [0.300,0.358]	0.124 [0.105,0.146]	0.374 [0.345,0.404]	0.514 [0.483,0.545]

Table 5: Hallucination rates with 95% Wilson score confidence intervals (computed over $N=1000$ prompts per model-relation pair).

G Controlling for output-space concentration

A key concern is that relation-level answer-space concentration (low entropy / high prior concentration) might jointly increase (i) the tendency to hallucinate and (ii) the apparent linearity proxy $\Delta \cos$. To probe this confound without additional supervision, we compute simple concentration proxies directly from the model outputs.

Answer-distribution concentration proxies. For each model m and relation r , let $\mathcal{A}_{m,r}$ be the multiset of answers among the $N=1000$ prompts that are labeled HALLUCINATION, and let $\mathcal{U}_{m,r}$ be the set of unique answers in $\mathcal{A}_{m,r}$ with $K_{m,r} = |\mathcal{U}_{m,r}|$. We compute (i) the Top-1 share, $\text{Top1}_{m,r} = \max_{a \in \mathcal{U}_{m,r}} \frac{\#(a)}{|\mathcal{A}_{m,r}|}$, and (ii) a normalized Shannon entropy (Shannon, 1948) over answers:

$$\text{Ent}_{m,r} = \frac{-\sum_{a \in \mathcal{U}_{m,r}} p(a) \log p(a)}{\log K_{m,r}}, \quad (13)$$

$$p(a) = \frac{\#(a)}{|\mathcal{A}_{m,r}|}.$$

We set both proxies to 0 when $|\mathcal{A}_{m,r}| = 0$, and define $\text{Ent}_{m,r} = 0$ when $K_{m,r} \leq 1$.

Partial correlation. Table 7 reports (within each model, $n=6$ relations) the association between relation-level linearity $\Delta \cos_{m,r}$ and hallucination rate $\hat{h}_{m,r}$ after *linearly controlling* for an output-space concentration proxy $z_{m,r} \in \{\text{Top1}_{m,r}, \text{Ent}_{m,r}\}$. Concretely, we residualize

both variables with an intercept:

$$\Delta \cos_{m,r} = \alpha_x + \beta_x z_{m,r} + \varepsilon_{m,r}^x, \quad (14)$$

$$\hat{h}_{m,r} = \alpha_y + \beta_y z_{m,r} + \varepsilon_{m,r}^y, \quad (15)$$

and define the *partial correlation* as the Pearson correlation $\text{corr}(\varepsilon_{m,r}^x, \varepsilon_{m,r}^y)$. The *unadjusted* correlation is the standard Pearson correlation between $\Delta \cos_{m,r}$ and $\hat{h}_{m,r}$ without this residualization.

For a pooled analysis over all 24 model \times relation points, we additionally include model fixed effects (model indicator variables) in the residualization design matrix, i.e., we regress $\Delta \cos$ and \hat{h} on (*intercept* + *model dummies* + z) and correlate the resulting residuals. This yields pooled partial correlations of $r = 0.778$ (Top-1 control) and $r = 0.808$ (entropy control). Overall, these results suggest that simple output-space concentration proxies do not explain away the observed relation-level $\Delta \cos$ -hallucination association.

H Rule-based judge baseline

We implement a deterministic regex-based baseline labeler for the two-class rubric. It labels an output as REFUSAL if it matches any of a small set of refusal templates (e.g., "I do not have information", "could not find", "not specified", "fictional", "cannot answer"), and otherwise labels it as HALLUCINATION. On the full set of 24,000 outputs, this baseline achieves 96.4% agreement with Gemini labels (Cohen's $\kappa = 0.928$). Label-wise precision and recall are reported in Table 8. We release the exact regex patterns (upon publication) to enable deterministic replication without external judge APIs.

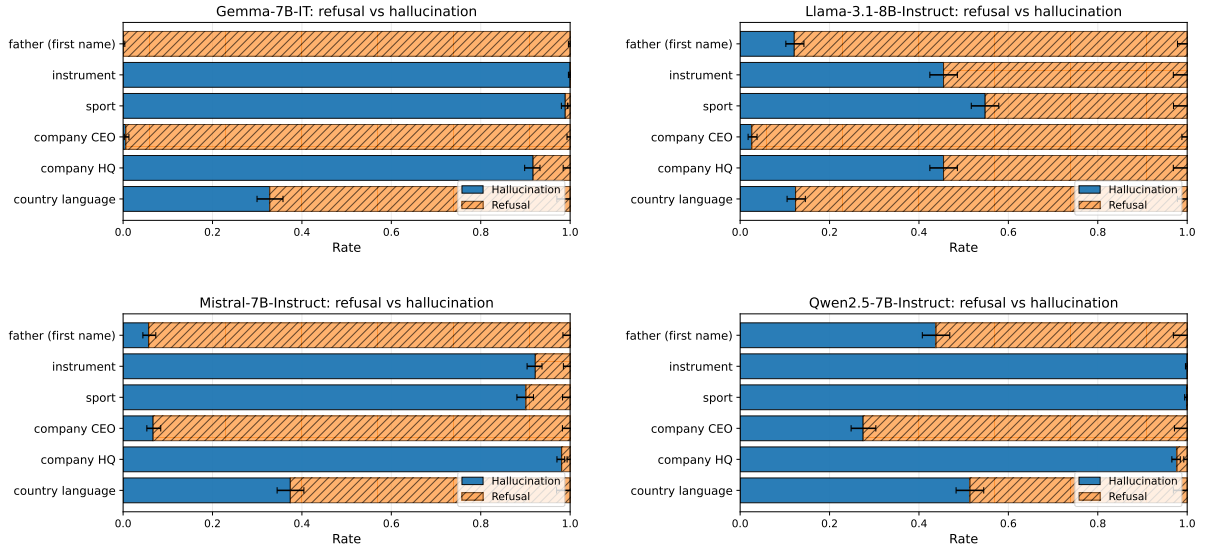


Figure 4: Per-relation behavioral outcomes under the standardized inference interface: hallucination (value-providing) vs. refusal rates with 95% Wilson score CIs, computed over $N=1000$ synthetic prompts per relation. This figure is a visual counterpart to Table 5.

Model	Pearson r	Spearman ρ	LOO range (r)	Exact perm. p (one/two)	Weighted r
Gemma-7B-IT	0.782	0.886	[0.714, 0.869]	0.038/0.071	0.811
Llama-3.1-8B-Instruct	0.817	0.841	[0.755, 0.923]	0.033/0.064	0.924
Mistral-7B-Instruct	0.799	0.600	[0.692, 0.914]	0.047/0.089	0.900
Qwen2.5-7B-Instruct	0.809	0.886	[0.754, 0.901]	0.038/0.086	0.868

Table 6: Robustness summaries for the within-model correlation between relation-level $\Delta \cos$ and hallucination rate ($n=6$ relations per model). Exact permutation p enumerates all $6!$ permutations; we report one-sided p for the directional alternative $r_{\text{perm}} \geq r_{\text{obs}}$ with the corresponding two-sided value (defined by $|r_{\text{perm}}| \geq |r_{\text{obs}}|$) after the slash. Weighted r uses weights proportional to the LRE held-out size n_{test} , downweighting relations with very small probe test sets.

Model	Pearson r	Partial r (Top-1)	Partial r (Entropy)
Gemma-7B-IT	0.782	0.732	0.798
Llama-3.1-8B-Instruct	0.817	0.736	0.673
Mistral-7B-Instruct	0.799	0.794	0.743
Qwen2.5-7B-Instruct	0.809	0.782	0.674

Table 7: Within-model partial correlations ($n=6$ relations) between relation-level $\Delta \cos$ and hallucination rate, controlling for simple answer-distribution concentration proxies computed from hallucinated outputs. Partial r is computed as the Pearson correlation between OLS residuals after regressing out the proxy (with intercept).

Label	Precision	Recall
REFUSAL	0.981	0.943
HALLUCINATION	0.949	0.983

Table 8: Agreement statistics between the deterministic regex baseline and Gemini labels on 24,000 outputs. Overall accuracy = 0.964 and Cohen's κ = 0.928.